Indian Journal of Engineering & Materials Sciences
Vol. 31, February 2024, pp. 51-57
DOI: 10.56042/ijems.v31i1.4887

A comparative investigation for flatness and parallelism measurement uncertainty evaluation using laser interferometry and image processing

Girija Moona[a,b*], Abhishek Singh[a], Sunder Bishnoi[c], Anju[a, b], Vinod Kumar[a], Rina Sharma[a, b] & Harish Kumar[d]

[a]Length, Dimension and Nanometrology, CSIR-National Physical Laboratory, Delhi 110 012, India

[b]Academy of Scientific and Innovative Research (AcSIR), CSIR-HRDC Campus, Ghaziabad 201 002, India

[c]School of Automation, Banasthali Vidyapith, Rajasthan 304 022, India

[d]National Institute of Technology, Delhi 110 036, India

Received: 14 August 2023; Accepted: 20 January 2024

Optical flats and parallels are precisely polished surfaces, customarily used as reference standards for quality assurance of fabricated components in numerous industries. In-line with the quality control, reliable flatness and parallelism measurements of optical flats and parallels through appropriate measurement methodologies are immensely significant. The present study describes a comparative investigation for flatness measurement of an optical flat with an effective diameter of 150 mm and parallelism measurement of an optical parallel with an effective diameter of 30 mm, through laser interferometry and image processing using MATLAB, followed by measurement uncertainty evaluation for perceptive and subjective confirmation of the measurement process. Outgrowths of both the approaches have been contemplated to be in significant congruence; the flatness value observed using laser interferometry is 120.50±30 nm whereas the flatness value observed using image processing is 118±32 nm. The parallelism values using laser interferometry is 0.44±0.009 arc second and using image processing is 0.36±0.01 arc second.

Keywords: Flatness, Parallelism, Interferometry, Image processing, Uncertainty

1 Introduction

Modern manufacturing targets elevated dimensional accuracy and geometrical tolerances of manufactured components to ensure their intended functioning. Flatness and parallelism are critical surface form characteristics and contribute extensively towards quality manufacturing. Hence, unerring, dependable, and traceable flatness and parallelism measurements are need of the hour. Optical flats and parallels are explicitly polished and lapped accurate standard artifacts, manufactured using optical grade glass and are used to measure the flatness and parallelism of micrometer anvils, assess various optical surfaces, to inspect gauge blocks/snap gauges, and characterize ring seals/valve seats, etc. They are placed close to the surface to be characterized and viewed with monochromatic light, the reflected light beams from the bottom surface of the optical flat or parallel and top surface of the test surface, interfere and produce an interference pattern. Primarily, the deviations in thickness of an air wedge originated from the sections between the optical flat/parallel and the test surface those are not in contact, influence the interference bands significantly. Furthermore, the shape of the interferogram visually demonstrates a contour map of the test surface for the interpretation of flatness and parallelism values[1]. In order to substantiate the traceability chain in measurement, flatness, and parallelism of optical flats and parallels respectively, can be precisely evaluated through a non-contact optical interferometry approach using a Fizeau interferometer, which is an interferometric arrangement with two reflecting surfaces placed facing each other. Two partially coherent laser beams are generated from the same source by amplitude division and are combined to form the interference pattern. Reflected light from the rear surface of the first transparent reflector is superimposed with the reflected light from the front surface of the second reflector to produce interference fringes, which exhibit the test surface profile with respect to the reference surface[2]. Image processing implicates the conversion of an image into digital composition, followed by carrying out specified operations on it, to embellish the image or to extract information. Variations in images during image

*Corresponding author (E-mail: moonag@nplindia.org)

processing are performed through designed algorithms. It is a diversified field associated with physics, mathematics, engineering, pattern recognition, artificial intelligence, and machine learning etc. A typical image processing appertains to; the importation of images from a digital camera, analysis, data compression, filtering, enhancement, and producing desired outputs. MATLAB: an abbreviation of 'matrix laboratory' is an advanced programming language for matrix computations, data plotting, algorithm implementation, and image processing in a faster pace; as compared to conventional programming languages. The MATLAB image processing toolbox (IPT) provides exclusive workflow applications and reference standard algorithms for the processing of images, analysis, algorithm development, and visualization. These comprehensive provisions can be utilized to carryout image enhancement, image segmentation, image registration, noise reduction, geometric transformations, and three-dimensional image processing operations[3]. Digital images consist of two or three-dimensional matrix of pixels, and distinct numbers associated with the pixels, demonstrate the grayscale or colour values assigned to them. The colour representation scheme of an image predominantly influences the image processing time and computational power. MATLAB supports several image files formats such as; BMP, GIF, HDE, JPEG, PCX, PNG, TIFF, and XWD, etc. There are explicit image processing functions in MATLAB as mentioned below[4]:

- To read and display an image 'imread' and 'imshow'
- To write the image 'imwrite'
- To check the contents of newly written file 'imfinfo', resize an image
- To resize an image 'imresize'
- To rotate an image 'imrotate'
- To crop an image 'imcrop'
- To get image pixel values (RGB value) 'impixel'
- Edge detection 'edge (image name, 'sobel') or edge (image name, 'canny')
- Noise reduction 'imnoise'

Edge detection is a fundamental part of image segmentation, a significant process in image analysis. The conclusiveness of image processing is based on the extent of perfection of edge detection. It is an image processing approach, to classify and locate specific boundaries, distinguished by immediate pixel concentration change within the image. Edge detection transforms actual images into edge images and substantially reduces the quantity of image data to be processed. Some of the common edge detection algorithms are Roberts, Sobel, Prewitt, Kirsh, Robinson, Marr-Hildreth, and Canny etc. A canny edge detector is a standard edge detection technique that finds image edges by separating noise from the original image, without tempering the edge features. In the present investigation, we have measured the flatness and parallelism values of optical flat and optical parallel respectively, using a Fizeau interferometer. Interferograms obtained from the CCD camera of Fizeau interferometer setup have further been processed in MATLAB for flatness and parallelism measurements through image processing. Particular ambiguities have consistently been affiliated with measurement observations due to numerous error sources. Identification of these error sources and estimation of their contribution in measurement outcomes becomes essential to evaluate the measurement uncertainty *i.e.*, parameter linked with measurement observations, that distinguishes dispersion of values that could be ascribed to the measurand. A comparative investigation has been carried out between physical measurements and image processing, followed by exhaustive measurement uncertainty evaluations for both techniques using the law of propagation of uncertainties (LPU/GUM) approach.

2 Materials and Methods

The Fizeau interferometer used in this experimental study: ZYGO's Verifire™ XPZ, as shown in Fig.1 (a), is equipped with a He-Ne laser (632.9 nm wavelength, Class II) and uses a phase shift interferometry technique. Here, a piezoelectric transducer provides movement to the reference element in forward and backward directions, generating constant phase variations between the reference wavefront and measurement wavefront. For flatness measurement, a reference flat is mounted on the main frame of the interferometer, and a test flat is mounted on separate adjustable receptacles, both emplaced facing each other, creating a cavity. This cavity is kept as small as possible, to limit the reverberations of air turbulence, and these two elements are aligned adequately. A laser beam exiting from the interferometer main frame aperture falls on the reference surface, which reflects a partial beam back to the interferometer creating a reference

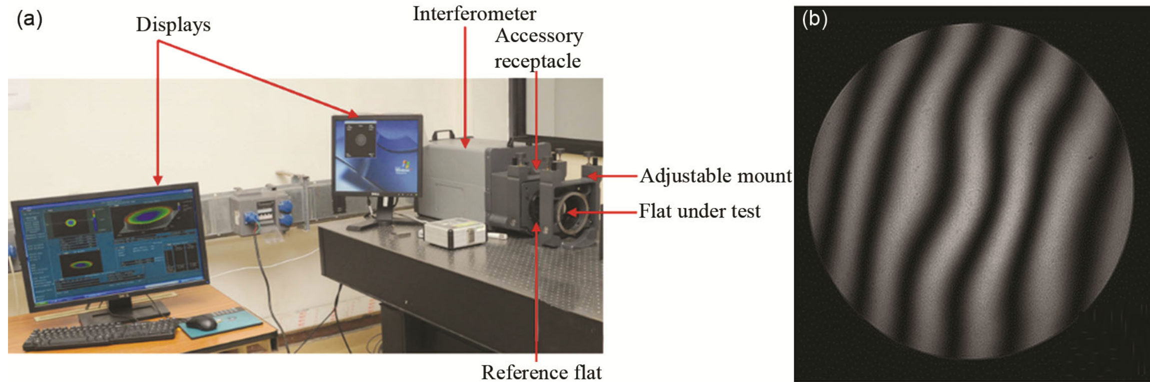

Fig. 1 — (a) Fizeau interferometer ZYGO's Verifire™ XPZ measuring flatness and (b) Interference pattern for flatness measurement.

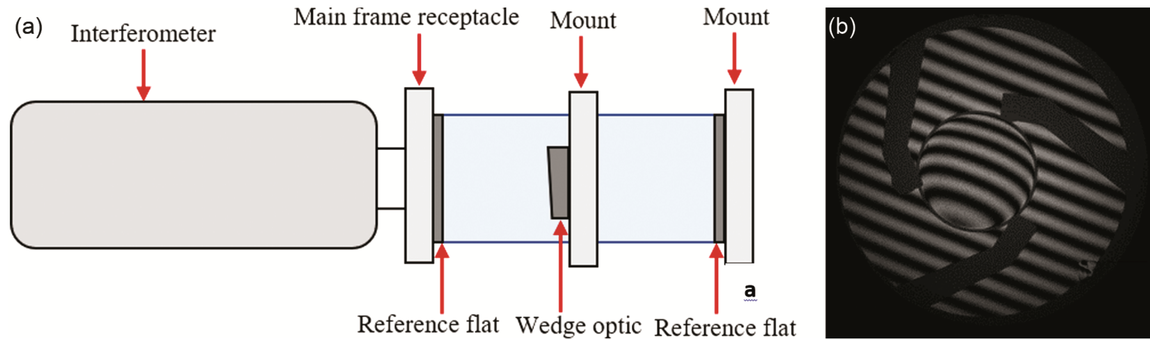

Fig. 2 — (a) Parallelism measurement setup and (b) Interference pattern for parallelism measurement.

wavefront. The residual laser beam from the reference surface is transmitted to the test surface and generates a measurement wavefront after getting reflected from the test surface. The reference wavefront and measurement wavefront are combined and interfere with each other, generating interference patterns, as displayed in Fig. 1(b). Fine-tuning is performed to minimize the number of fringes *i.e.*, nulling the fringes. During measurement, the Fizeau interferometer cavity length is modulated in a precise manner and a 640 × 480 pixels CCD camera captures several interferogram images to be analyzed by the software (MetroPro™ software). Flatness represents the surface deviation between two parallel planes, it is the condition of a surface with all the elements lying in one plane, whereas parallelism is estimated with respect to a reference plane, it is the condition of a surface or line with equidistant elements from the datum. For parallelism measurement, the cavity is created through two reference flats, one mounted on the interferometer main frame and other on an independent adjustable mount. The optical parallel (wedge optic) to be tested for parallelism, is inserted in the cavity, as shown in Fig. 2(a). An interferogram is obtained from the reference and measurement

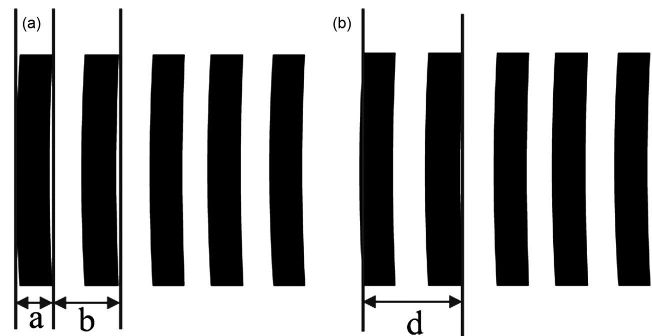

Fig. 3 — Estimation from the fringe pattern (a) Flatness measurement and (b) Parallelism measurement.

wavefronts, as shown in Fig. 2(b) and parallelism measurements are done after fringe nulling. The phase difference of the interference pattern can be determined using an algorithm, eventually computing the flatness and parallelism of the test surface. Here, the form characterizations of test surfaces are carried out relative to the reference surfaces, hence the measurement accuracy extensively depends on reference surface attributes[5-6].

Image processing of interference patterns as shown in Fig. 3, was performed for flatness and parallelism measurements using MATLAB, using Eq. (1) & (2) respectively[5].

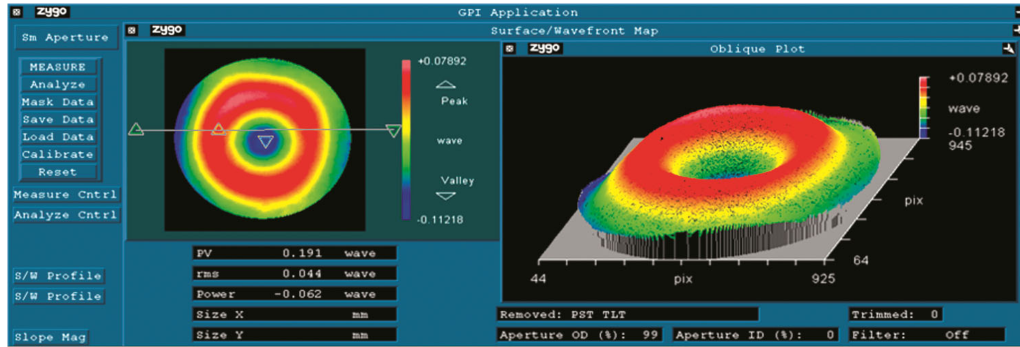

Fig. 4 — Flatness measurement wavefront map.

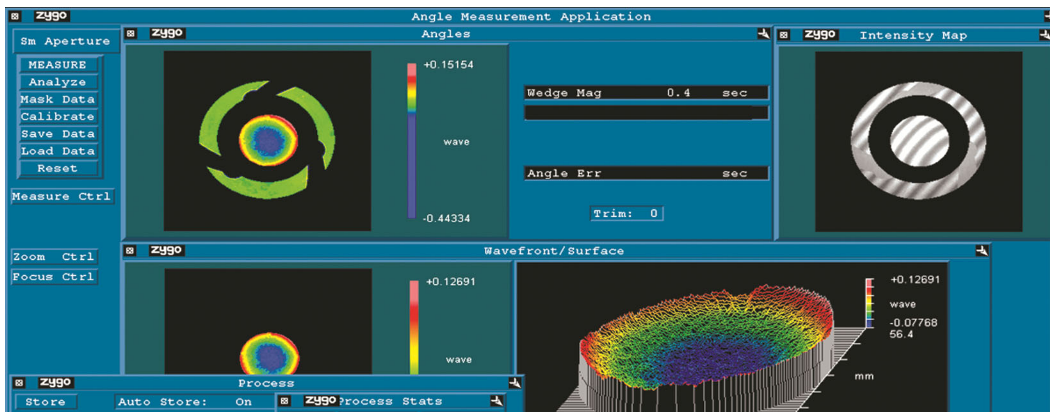

Fig. 5 — Parallelism measurement wavefront map.

$$Flatness\,error\ (nm) = \left(\frac{a}{b}\right) \times \left(\frac{\lambda}{2}\right) \quad \ldots(1)$$

Here, a: Peak deviation
b: Fringe spacing
λ: Laser wavelength (632.9 nm)

$$Parallelism\,a\ (arcsec) = \frac{\lambda}{2 \times n \times d \times 0.000005} \quad \ldots(2)$$

Here, λ: Laser wavelength (632.9 nm)
n: Refractive index
d: Distance between two consecutive bright or dark fringes

3 Results and Discussion

The present investigation was performed to measure flatness and parallelism using a laser interferometer and the outgrowths were compared with image processing results using MATLAB. The environmental conditions maintained during measurement are specified below:

Temperature: 20 ± 0.2°C
Relative humidity: 50 ± 10%

Flatness measurement observations for an optical flat with an effective diameter of 150 mm, using a laser interferometer are demonstrated in Fig. 4 and Table 1.

Table 1 — Flatness observations

Sl. No.	Flatness PV Wave	Flatness RMS Wave	Flatness (nm) *Calculated using flatness PV wave values, with wavelength 632.9 nm
1	0.189	0.043	119.62
2	0.190	0.043	120.25
3	0.190	0.043	120.25
4	0.190	0.043	120.25
5	0.189	0.043	119.62
6	0.191	0.0.43	120.88
7	0.192	0.043	121.52
8	0.191	0.043	120.88
9	0.191	0.044	120.88
10	0.191	0.044	120.88
Average flatness	0.190	0.043	120.50
Standard deviation	0.001	0.000	0.61

Parallelism measurement observations for an optical parallel of an effective diameter of 30 mm, using a laser interferometer are demonstrated in Fig. 5 and Table 2.

Interference patterns obtained by the CCD camera of the Fizeau interferometer were subjected to image processing through MATLAB, using a Canny edge detector, for computations of flatness and parallelism in accordance with equations 1 and 2[7]. Figures 6 (a & b) display the MATLAB image processed flatness and parallelism fringe patterns. Tables 3 and 4 exhibit the parameters evaluated through image processing for flatness and parallelism estimations, respectively.

Possible error sources associated with both measurement techniques have been identified and demonstrated in fishbone diagrams in Fig.7 and 8[8-9].

Table 2 — Parallelism observations

Sl. No.	Parallelism (Wedge magnification) (arc second)
1	0.45
2	0.43
3	0.43
4	0.43
5	0.42
6	0.44
7	0.44
8	0.45
9	0.45
10	0.44

Average parallelism =0.44 arc second
Standard deviation= 0.01 arc second

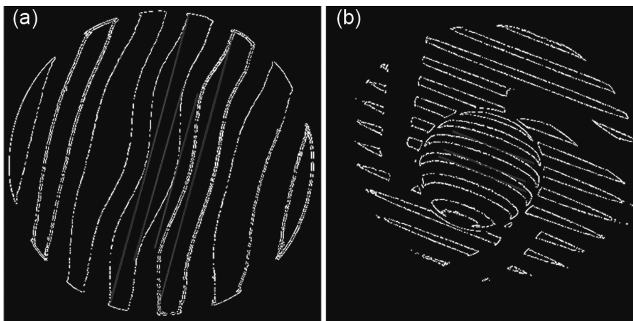

Fig. 6 — Image processed in MATLAB (a) for flatness measurement and (b) for parallelism measurement.

Detailed uncertainty budgets for flatness and parallelism measurements in accordance with the JCGM recommendations[10-12] have been presented in Tables (5-8).

The two techniques incorporated for flatness and parallelism estimations of optical flat and optical parallel respectively, are observed to dwell in a reasonable concurrence in terms of measured average values and measurement uncertainties.

Table 3 — Image processing observation for flatness using MATLAB

Sl. No.	Peak deviation 'a' (Pixels)	Fringe spacing 'b' (Pixels)	Flatness estimated using equation 1 (nm)
1	52	139	118.15
2	52	140	117.07
3	55	146	119.02
4	52	140	117.67
5	51	139	117.12
6	51	139	117.05
7	52	139	118.41
8	52	139	118.74
9	51	139	117.23
10	51	137	118.82

Average flatness = 118 nm
Standard deviation = 0.79 nm

Table 4 — Image processing observation for parallelism using MATL33AB

Sl. No.	Distance b/w consecutive bright or dark fringes d (Pixels)	Parallelism α estimated using equation 2 (arc second)
1	459	0.36
2	451	0.37
3	459	0.36
4	466	0.35
5	467	0.35
6	470	0.35
7	461	0.36
8	458	0.36
9	459	0.36
10	460	0.36

Average parallelism = 0.36 Arc Second
Standard deviation = 0.006 Arc Second

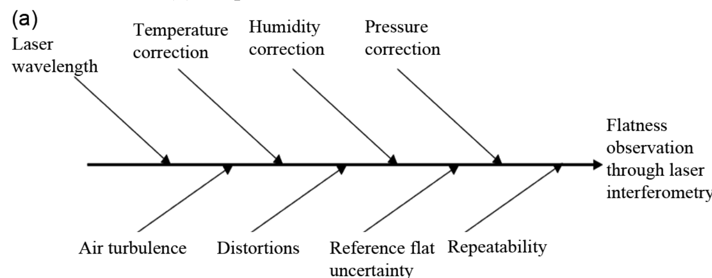

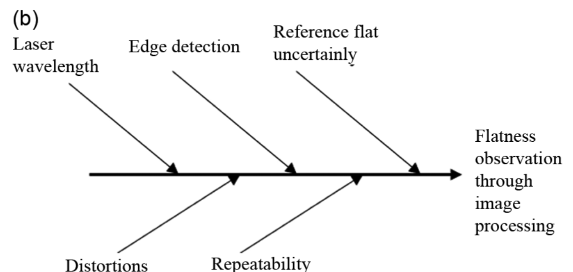

Fig. 7 — Error sources in flatness measurement (a) through laser interferometry, and (b) through image processing.

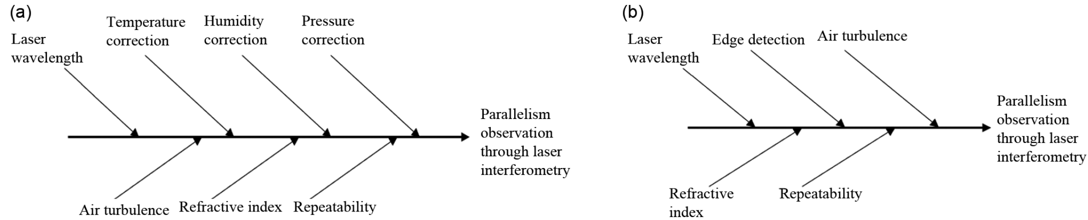

Fig. 8 — Error sources in parallelism measurement (a) through laser interferometry and (b) through image processing

Table 5 — Uncertainty budget for flatness evaluation through laser interferometry

Sources of error	Limits	Type	Probability distribution	Degree of freedom	Standard uncertainty	Sensitivity coefficient	Uncertainty contribution (µm)
Laser wavelength (µm)	0.00001	B	Normal	∞	5.00E-06	1	5.00E-06
Temperature correction (°C)	1	B	Rectangular	∞	0.5774	1.00E-06	5.77E-07
Humidity correction (% RH)	10	B	Rectangular	∞	5.7735	1.00E-08	5.77E-08
Pressure correction (mm of Hg)	10	B	Rectangular	∞	5.7735	3.33E-07	1.92E-06
Air turbulence (µm)	0.002	B	Rectangular	∞	0.0012	1	1.15E-03
Distortions (µm)	0.02	B	Rectangular	∞	0.0115	1	1.15E-02
Reference flat uncertainty (µm)	0.02	B	Normal	∞	0.0100	1	1.00E-02
Repeatability (µm)	0.0002	A	Normal	9	0.0002	1	2.04E-04

Combined uncertainty = ±0.015 µm

Expanded uncertainty at 95% confidence interval (coverage factor k=2) = ±30 nm

Table 6 — Uncertainty budget for flatness evaluation through image processing

Sources of error (µm)	Limits	Type	Probability distribution	Degree of freedom	Standard uncertainty	Sensitivity coefficient	Uncertainty contribution (µm)
Laser wavelength	0.00001	B	Normal	∞	5.00E-06	1	5.00E-06
Edge detection	0.01	B	Rectangular	∞	0.0058	1.00E+00	5.77E-03
Reference flat uncertainty	0.02	B	Normal	∞	0.0100	1	1.00E-02
Distortions	0.02	B	Rectangular	∞	0.0115	1	1.15E-02
Repeatability	0.0003	A	Normal	9	0.0000	1	2.88E-05

Combined uncertainty = ±0.016 µm

Expanded uncertainty at 95% confidence interval (coverage factor k=2) = ±32 nm

Table 7 — Uncertainty budget for parallelism estimation through laser interferometry

Sources of error	Limits	Type	Probability distribution	Degree of freedom	Standard uncertainty	Sensitivity coefficient	Uncertainty contribution (Arc Second)
Laser wavelength (µm)	0.00001	B	Normal	∞	5.00E-06	1	1.03E-06
Temperature correction (°C)	1	B	Rectangular	∞	0.5774	1.00E-06	1.19E-07
Humidity correction (% RH)	10	B	Rectangular	∞	5.7735	1.00E-08	1.19E-08
Pressure correction (mm of Hg)	10	B	Rectangular	∞	5.7735	3.33E-07	3.96E-07
Air turbulence (µm)	0.002	B	Rectangular	∞	0.0012	1	2.38E-04
Refractive index (µm)	0.025	B	Rectangular	∞	0.0144	1	2.98E-03
Repeatability (arc sec)	0.003	A	Normal	9	0.003	1	3.44E-03

Combined uncertainty = ±0.005 Arc Second

Expanded uncertainty at 95% confidence interval (coverage factor k=2) = ±0.009 Arc Second

Table 8 — Uncertainty budget for parallelism estimation through image processing

Sources of error	Limits	Type	Probability distribution	Degree of freedom	Standard uncertainty	Sensitivity coefficient	Uncertainty contribution (Arc Second)
Laser wavelength (µm)	0.00001	B	Normal	∞	5.00E-06	1	1.03E-06
Edge detection (µm)	0.03	B	Rectangular	∞	0.0173	1	3.57E-03
Air Turbulence (µm)	0.002	B	Rectangular	∞	0.0012	1	2.38E-04
Refractive Index (µm)	0.025	B	Rectangular	∞	0.0144	1	2.98E-03
Repeatability (arc sec)	0.002	A	Normal	9	0.002	1	1.57E-03

Combined uncertainty = ±0.005 Arc Second

Expanded uncertainty at 95% confidence interval (coverage factor k=2) = ±0.01 Arc Second

4 Conclusion

The present investigation delineates the detailed process of flatness and parallelism measurements of optical flat and optical parallel, through laser interferometry and image processing using MATLAB, followed by measurement uncertainty evaluations, adopting the law of propagation of uncertainties approach. Flatness values estimated through laser interferometry and image processing were 120.50 nm and 118 nm respectively, while the parallelism values assessed through laser interferometry and image processing were 0.44 Arc Second and 0.36 Arc Second. Numerous indispensable error sources, contributing during the measurement procedure, were identified and measurement uncertainties were evaluated in accordance with the JCGM recommendations. Measurement uncertainties estimated for flatness measurement using laser interferometry and image processing were ±30 nm and ±32 nm respectively, whereas corresponding uncertainties for parallelism measurement were ±0.009 Arc Second and ±0.01 Arc Second, at 95% confidence interval (coverage factor k=2). Measurement outcomes acquired from both methodologies appeared to be in plausible agreement.

Acknowledgment

The authors are very thankful to the Director, CSIR-National Physical Laboratory, India for his continuous encouragement and support.

References

1 Xu C, Chen L & Yin J, *Appl Opt*, 48(13) (2009) 2536.
2 Bhattacharyya D, Ray A, Dutta B K & Ghosh P N, *Opt Laser Technol*, 34(1) (2002) 93.
3 Chaudhary K P, Shakher C & Shashi K, *Mapan-JMSI*, 26(1) (2011) 15.
4 Abo-Zahhad M, Gharieb RR, Ahmed S M & Donkil A A, *J signal inf process*, 5(04) (2014) 123.
5 Hibino K, Oreb B F, Fairman P S & Burke, *Appl Opt*, 43(6) (2004) 1241.
6 Sykora D M & Holmes M L, *Proceedings SPIE Optical Metrology 8082 80821R*, (2011).
7 Xin G, Ke C &Xiaoguang H, *IEEE 10th International Conference on Industrial Informatics*, (2012) 113.
8 Wirotrattanaphaphisan K, Buajarern J & Butdee S, *J of Phy: Conference Series*, 1183 012009 (2019).
9 Bitou Y, Takatsuji T & Ehara K, *Metrologia*, 45(1) (2008) 21.
10 JCGM 100: 2008 (2008) Evaluation of Measurement Data – Guide to the Expression of Uncertainty in Measurement, Bureau International Des Poids Et Mesures, France
11 Moona G, Sharma R, Kiran U & Chaudhary K P, *Mapan-JMSI*, 29(4) (2014) 261.
12 Takatsuji T, Osawa S, Kuriyama Y & Tomizo K, *Proceedings. SPIE Optical Science Technol*, (2003).